

FINITE ELEMENT ANALYSIS OF GEAR WIDTH INFLUENCE ON THE MESHING STIFFNESS AT HELICAL GEARS

Ionel Sorin GABROVEANU, Andrei TUDOR, Radu MIRICA, Sorin CANANAU

This paper presents the results of a theoretical study on the stiffness behavior in a helical gear meshing teeth and the influence of overlap ratio on vibratory behavior. The theoretical and experimental research results could lead to practical results of interest for industrial applications. In the present study, the focus was on static meshing simulation. By using the finite elements method it was possible to simulate static engagement and stiffness values were obtained for every point considered on the line of contact. Using this method, it was possible to obtain the values of the meshing stiffness as an important in the behavior of helical gear meshing.

Keywords: helical gear, stiffness, Finite Elements Method

1. Introduction

Researches on teeth deformations in meshing (and therefore their stiffness behavior under load) have progressed with the development of mechanical gears manufacturing and the development of improved devices for measurement and control of mechanical systems.

Among the first works concerning the stiffness but also the elastic deformation of teeth gears under load, one can note those made by Weber and Banaschek [1], Rettig [2,3], and Schlaf [4]. Concerning the first models used, the beam model is embedded. This is justified by practical results and is in accordance with experiments. Moreover, it can be adapted relatively easily from spur to helical gears, also with good results, [5]. Concerning the vibrations under load of gear shafts as part of operating mechanical transmission, Knabel [6] found that the bending vibrations are dominant especially in domain of high rotational speeds, considerably higher than the resonant gear set frequency (teeth frequency).

An original method to define the stiffness was formulated by Dobre [7], who considered the early and late meshing of spur gears, by so-called functional clearances. It was shown that the variation of meshing stiffness between the different meshing areas is not sudden (Fig. 1), according to experiments provided by Rettig [2].

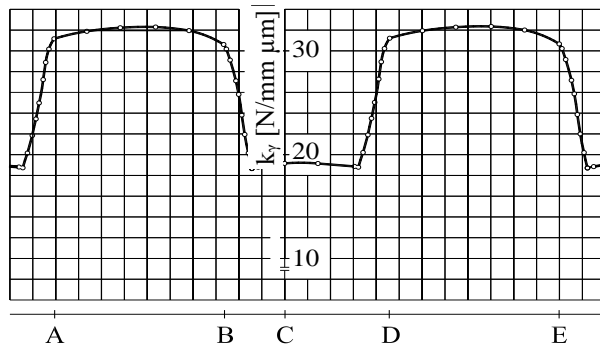


Fig. 1. Stepped static variation of mesh stiffness along the meshing line at spur gears (after Dobre, [7]):

$$a = 125\text{mm}; m = 4\text{mm}; \beta = 0^\circ; z_1 = 23; z_2 = 37; x_1 = 0,69; x_2 = 0,733; b = 46\text{mm}; T_1 = 784,4$$

Palermo *et al.* [8] have studied the estimating possibility of gearbox noise, as a way to achieve a high level research project at low testing needs. The method is based on calculation of total dynamic error, DTE, using the total static error, STE. By dedicated software, LMS Virtual Lab Motion, coupled with a program for gearing analysis they obtain the dynamic behavior of gear.

According to studies of Van Khang Nguyen *et al.* [9], the fundamental characteristics of gear vibration are the frequency, the harmonics and the sub-harmonics due to modulation effects. The sub-harmonics can be used as diagnostic elements to detect the gear damages. A comparison between the model and the experimental data obtained on a test bench was performed. Chee Keong Tan and David Mba [10] have studied the ability to diagnose the wear degree of gears and their accuracy by repeatable and reliable methods.

Liu Jian *et al.* [11] attacked the problem of total gear meshing deviation using the gear noise as a measurable parameter in operation. The paper focuses on the assessment of the total deviation and on possible ways to reduce this. In [12], the influence of the operating conditions on the gear noise emission levels was studied.

In [13], work regarding tooth deflection and their effects using the Finite Element Method (FEM) was performed with good agreement with existing gear standards.

It is well known that FEM can be tedious and time-consuming; opposite, analytical methods considered as efficient as FE analysis have been proposed by researchers. One of the most visible methods, the Rayleigh–Ritz energy method, was applied by Hwa Yau [14] in order to investigate the shear effect on involute gear teeth. Based on the model of Weber and Banaschek [1], an improved model that considers the fillet-foundation stiffness was proposed by Chen and Shao [15] in order to investigate the meshing stiffness of various crack types but the part

between the root circle and base circle was not taken into account. The method of potential energy was presented by Yang and Lin [16]. They were able to calculate the mesh stiffness effectively. More recently, Bruyère *et al.* [17] have studied the profile modifications in order to minimize transmission error variations in narrow-faced spur helical gears. They proposed formulae which rely partly on the theoretical results obtained when using constant mesh stiffness per unit contact length.

Also, Jabbour and Asmar [18] have calculated tooth stress of metal helical gear taking into account non uniform load distribution along the lines of contact. A new, modern adaptive grid-size FE modeling helical gear, with direct correlation to mesh stiffness of helical gears was developed by Barbieri *et al.* But the NURBS description could be improved for obtaining the gear profile.

2. FEM models

The numerical analysis of tooth stiffness was made on many FE models. The FE models approximate geometrical 3D contact representations of structures that must be solved. Because automatic algorithms that transform the problem of material resistance into a FE model are not available, the implication of human operator is essential. For a specific geometric structure, one can generate many FE models, all of them correct, however having different performances from different points of view.

The detailed master model, the base for other FE models (of a gear set) is shown in Figure 2. For this model, the helical gear set having the data given into Table 1 was used. This is an involute helical gear having the overlap ratio equal to 1 (i.e. $\varepsilon_\beta = 1$). The pinion torque of this basic FE model was determined using the load capacity - based on pitting and tooth root crack - conforming to ISO 6336-2:2006 and ISO 6336-3:2006.

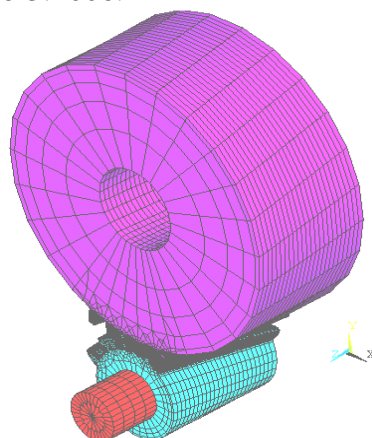


Fig. 2. The detailed basic, discrete FEM model

In order to emphasize the variation manner of gear stiffness, many gear set FEM models - derived from the basic FEM model presented above - having the overlap ratio nearly 1 have been used (Figure 3). These models are different from the basic one by:

- constructive solution of pinion shaft (tubular or full);
- number of finite elements on face width;
- teeth number build on wheel and pinion.

Table 1.

Base data on studied gear into different FEM models

Description	Symbol	Value
Centre distance	a_w	125 mm
Teeth number of pinion	Z_1	15
Teeth number of wheel	Z_2	46
Helix angle	β	10°
Profile shift coefficient of pinion	x_1	0.427
Profile shift coefficient of wheel	x_2	-0.138
Face width	b	72.3668 mm
Transverse contact ratio	ϵ_α	1.45318
Overlap ratio	ϵ_β	1
Base torque applied on pinion	T_1	392.466 N·m

The characteristics of FEM models from Figure 3 are given in Table 2. In order to reduce the dimensions of the model, only five teeth were generated on wheel and on pinion. The number of elements on the radial direction was correlated with the one on the face width in order to obtain elements having comparable dimensions of the three sides.

Table 2.

Characteristics of discrete FEM models

Model	Number de elements one face width	Number of nodes	Number of elements
Figure 2	25	129983	27050
Figure 3, a	12	179326	40548
Figure 3, b	8	142908	32424
Figure 3, c	25	338235	70300
Figure 3, d	50	129983	27050
Figure 3, e	100	955065	222080
Figure 3, f	25/60	159740	33600

The mesh is automatically generated after setting the parameters of FEM models but there are also models with specific mesh design. For contact elements, the declaration of contact and the indication of contact surfaces are necessary. After model generation - if there are no messages that indicate geometrical lack of convergence (too sharp angles, too big ratios between the sides of generated

elements) that can cause calculus errors - the model is validated and can be solved.

The FEM models discussed in this paper use currently buffer files which have approximately 16 GB, using the ANSYS program. Other programs utilize bigger buffer files.

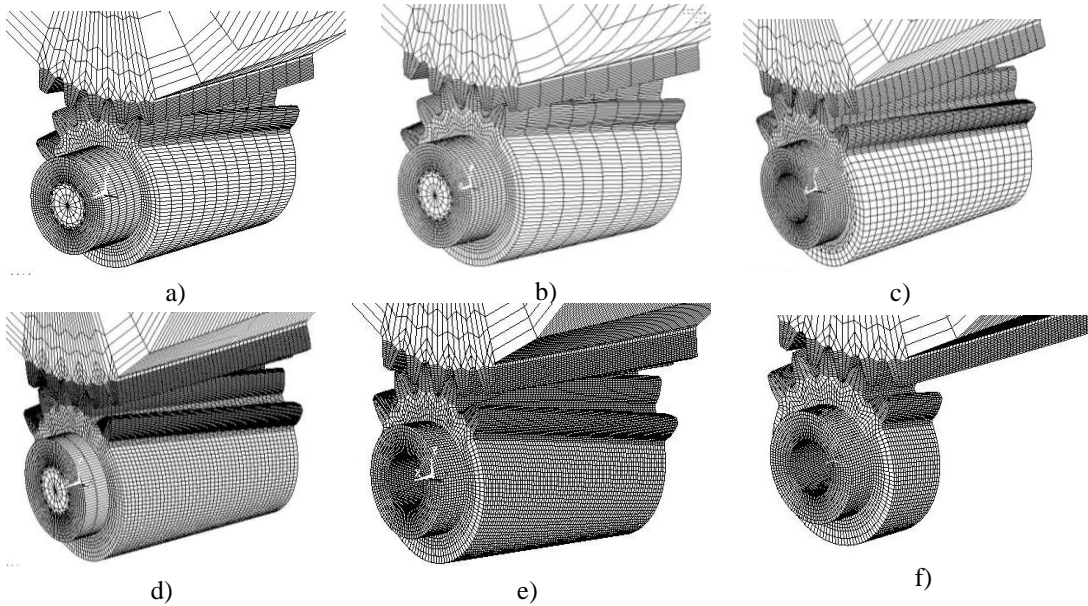


Fig. 3. Gear set FEM models (s. Table 2):

a) full pinion, 12 elements on gear width; b) full pinion, 8 elements on gear width; c) tubular pinion, 8 element on gear width; d) full pinion, 50 elements on gear width; e) tubular pinion, 100 elements on gear width; f) normal wheel, narrow pinion, 25 elements on width of pinion and 60 on wheel width.

3. Contact positions and FEM modeling

The FEM models are analyzed in the meshing points shown into Figure 4.

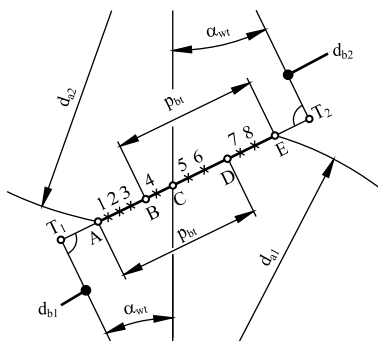


Fig. 4. Analyzing positions on meshing line of contact points of teeth flanks

In addition to characteristic points on meshing line - the points on path of contact (line of action) A ... E - other eight points are considered along the path of contact. The distances between these points and point A of theoretical beginning of contact path are given in Table 3.

Here, the calculated maximum theoretical contact point is added. The bringing of toothed wheels of FEM model in contact in these above mentioned points is made by rotation with the angles given into Table 3. These angles are used for positioning the gears, starting from the original generating position. On the axis of central tooth (in transversal plane) each wheel-model is superimposed on the line of centers. In this manner, the model components are brought in the necessary contact position and allow passing into next stage of final FEM model building.

Table 3.

Positions of calculating point on meshing line and associated characteristics

Point	Distance on meshing line [mm]	Calculated depth displacement [μm]	Rotation angle of pinion to be brought into considered point [rad]	Rotation angle of wheel to be brought into considered point [rad]
A	0	2.75	-0.351082	0.046188
1	0.7125	2.89	-0.325983	0.038003
2	3.2194	2.87	-0.238490	0.009473
3	5.2182	2.11	-0.168496	-0.013351
B	5.4244	4.18	-0.161253	-0.015713
4	5.9166	3.36	-0.143998	-0.021340
C	6.5465	2.19	-0.121983	-0.028518
5	8.7186	3.74	-0.046006	-0.053294
6	11.2165	2.75	0.041487	-0.081824
D	11.9689	2.75	0.067797	-0.090403
7	14.7169	2.67	0.163977	-0.121766
8	16.2172	2.24	0.216473	-0.138884
E	17.3933	2.75	0.257626	-0.152304

4. Declaration of contacts

After defining mesh modeling into working position by rotating wheels, we proceed to declaration of contacts. The ANSYS software has a special module dedicated to declaration of contacts and their type.

The contact can be classified according to the following points of view:

- friction in adjacent meshing structure (taking into account tangential forces);
- modification of contact surface at load application;
- material behaviour;
- displacement of nodes and elements in contact.

The studied contacts from this paper have the following characteristics:

- are without friction;
- a certain value of depth displacement of nodes (a lack of FE method) is admissible, but this is evaluated from the point of view of physical sense;
- the elastic behavior of materials in contact is admissible;

By bringing the surfaces in contact, initial elastic contact deformation appear. These are interferences caused by geometrical irregularities of surfaces into contact of the discrete FEM model. Figure 5 shows the surfaces into contact for one of considered cases from Figure 3. Here the variation of displacements is not taken into account because these are too small in comparison with the elastic displacements.

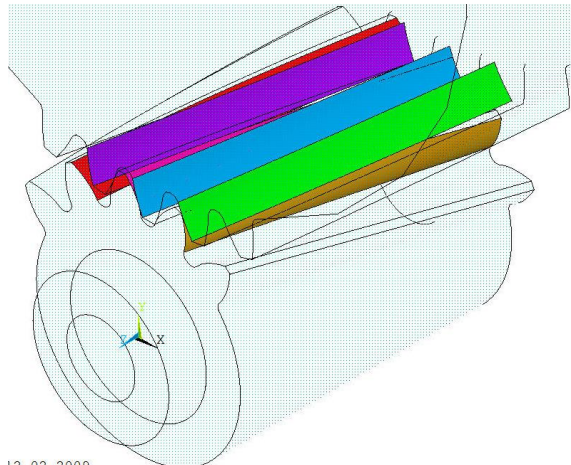


Fig. 5. Flank surfaces (emphasized with different colors) in meshing point C:
the displacement values have too small variations and remain unobservable

The usual methods for solving of nonlinear contact problems are the method of penalty functions and the method of Lagrange multipliers, followed by iterations using the Newton-Raphson algorithm. The method of penalty function has as an essential disadvantage - the appearance of penetrations between both surfaces into contact (or on the contrary it can lead to numerical instabilities). The method of penalty functions introduces no supplementary variables into system, but the method of Lagrange multipliers introduces such variables (i.e. the contact forces) and can lead to a singular stiffness matrix. Usually, the optimum compromise is accepted: the contact problem is solved using a combination of penalty functions completed with Lagrange multipliers.

5. Results – Gear meshing stiffness

1. The tooth flank surface was generated by helical extrusion of a high order spline curve obtained by simulating the evolventic tooth generation process.

Such a generation method of the FE model is affected by inherent errors. What is very important, is that the obtained initial interference of tooth flanks - caused by model generation - is 20 times smaller than the elastic deformation of teeth. Thus, the errors caused by this interference are drastically limited.

2. The value of penetration is generally less than 1 μm with local maxima below 4 μm appearing into domains where the contact pressure is elevated. Taking into consideration that the roughness amounts to 2 μm for grinded flanks, we consider that the precision of obtained results is acceptable.
3. The contact lines (Figure 6) can be emphasized only where the contact pressures are shown. For example, because of the extremely small displacements, the contact lines can not be observed on Figure 5.

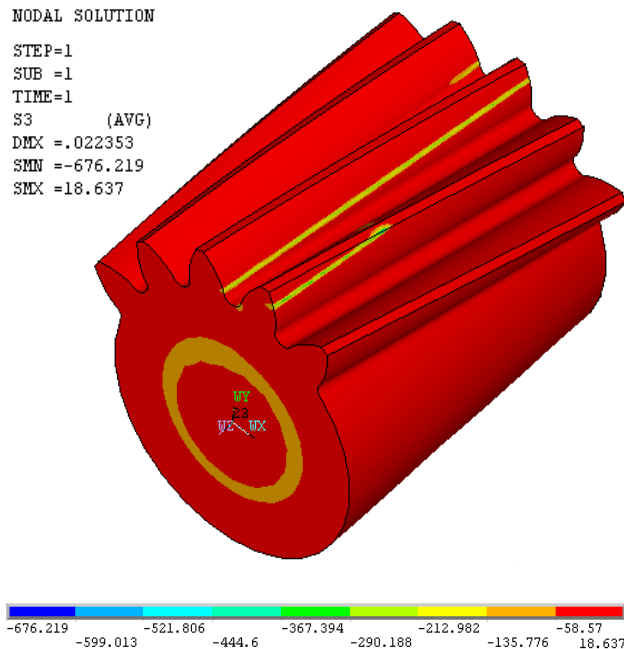


Fig. 6. Distribution of principal stress σ_3 , for pinion into meshing point 2:
 only contact lines are visible

4. The total length of the obtained contact lines (contact pattern) is constant with an approximate value of $1.5 \cdot b$ (b is the face width dimension).
5. The stiffness in median section of gear $k_t = M_t / \phi_{12}$ (valid only for the considered torque because the contact deformations are not linear) amounts to 700 kNm/rad, approximately the same value for all points on the action line, as it is shown in Figure 7. The transversal displacement at tooth root divided by the root radius dimension of the pinion amounts to $\phi_{12} \approx 0.015/27.17$ rad

that means $\varphi_{12} \approx 0.03^\circ$. The total displacement varies between 0.02228 mm to 0.02367 mm that means the maximum node displacement varies with 6.2% for a given load. This allows to conclude that the meshing stiffness is almost constant during meshing process, in the case of the overlap ratio equal to unity.

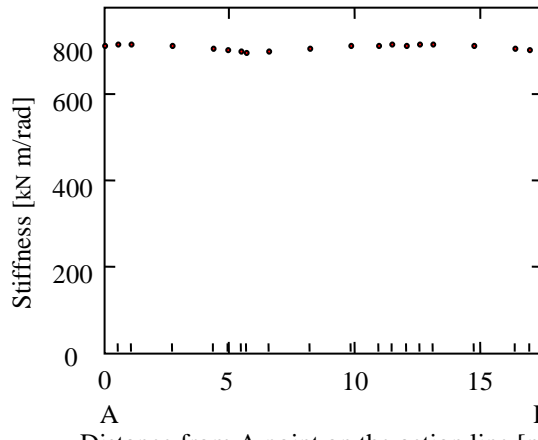


Fig. 7. Static stiffness in meshing along the action line, mediate on cylinder of 40 mm

6. Conclusions

1. A short overview of problematic of noise reducing of gearboxes is made. A quasi-constant stiffness is a way to solving this problem. The study of mesh stiffness of helical gears can be made successfully using FE analysis.
2. The FE model was built and used to study the influence of the overlap ratio on the stiffness variation. More FE models having the overlap ratio equal to unity were analyzed with the software ANSYS. The meshing was modeled in more points on the meshing line i.e. the characteristic points (A ... E) of path of contact (or line of action) and another intermediary eight points (situated between A and E).
3. Some important observations on realizing the FE model to simulate the meshing were made. The dimensions of elements are approximately equal on the three directions. Some inherent errors to contact modeling produce a “penetration” of modeled flanks of pinion and wheel. This “penetration” must be smaller than the flank roughness and represents a quality measure of model. The FEM nonlinear contact problem is solved using a combination of penalty functions completed with Lagrange multipliers. The rotational angle of the pinion is obtained by integration on a cylinder having the diameter smaller as tooth root diameter.
4. The obtained displacements are small and cannot emphasize the contact lines, but these ones can be emphasized by distribution of principal stresses.

5. The FE model of gear set, whith the overlap ratio equal to unity has proved the extremely small variations of meshing stiffness. In the future, the variation of the meshing stiffness for a gear set having overlap ratio equal to 2 will be studied.

R E F E R E N C E S

- [1] *C. Weber, K. Banaschek*, Formänderung und Profilrücknahme bei gerad-und Schrägverzahnten Rädern. Schriftenreihe Antriebstechnik, nr. 11, Vieweg, 1953
- [2] *H. Rettig*, Dynamische Zahnkraft. Diss. TH München, 1957
- [3] *H. Rettig*, Innere dynamische Zusatzkräfte bei Zahnradgetrieben. Antriebstechnik, 16 (1971), nr. 11, 655-663.
- [4] *G. Schlaf*, (1962). Beitrag zur Steigerung der Tragfähigkeit und Laufruhe geradver-zahnter Stirnräder durch Profilrücknahme. Diss. TU Dresden.
- [5] *H. Ziegler*, Verzahnungssteifigkeit und Lastverteilung schrägver-zahnter Stirnräder. Diss. TH Aachen, 1971.
- [6] *W. Knabel*, Geräusche und Schwingungen an Stirnradgetrieben. Diss. TU München. 1976.
- [7] *G. Dobre*, Contribuții privind influența factorilor constructivi și tribologici asupra reducerii zgomotului angrenajelor cilindrice. Institutul Politehnic din București, 1987 (In Romanian).
- [8] *A. Palermo, D. Mundo, A.S. Lentini, R. Hadjit, P. Mas, W. Desmet*, Gear noise evaluation through multibody TE-based simulations, ISMA2010 Noise and Vibration Engineering conference, Leuven (Belgium), 20-22 September 2010
- [9] *Khang Nguyen, Manh Cau Thai, Phong Dien Nguyen*, Modelling parametric vibration of gear-pair systems as a tool for aiding gear fault diagnosis. Technische Mechanik 24 3-4 198 205, 2004
- [10] *Chee Keong Tan, David Mba*, Identification of the Acoustic Emission source during a comparative study on diagnosis of a spur gearbox, Tribology International, Vol.38, Issue 5, 469-480, (2005)
- [11] *Liu Jian, Wang Zhaobing, Wu Hongji, Chen Chiping*, Single flank total composite error analysis and noise prediction of gears, Precision Engineering, Vol.9, Issue 2, 83-90, 1987
- [12] *RIR Hamzah, KR Al-Balushi, D Mba*, Observations of acoustic emission under conditions of varying specific film thickness for meshing spur and helical gears, Journal of Tribology 130 (2), 021506
- [13] *R. Muthukumar, M.R. Raghavan*, Estimation of gear tooth deflection by the finite element method, Mechanism and Machine Theory, Vol. 22, Issue 2, 177–181, 1987
- [14] *Hwa Yau*, Analysis of Shear Effect on Gear Tooth Deflections Using the Rayleigh-Ritz Energy Method, Ohio State University, 1987, 187-213
- [15] *Z. Chen, Y. Shao*, Dynamic simulation of spur gear with tooth root crack propagating along tooth width and crack depth, Eng. Fail. Anal. 18 (2011) 2149–2164.
- [16] *D. Yang, J. Lin*, Hertzian damping, tooth friction and bending elasticity in gear impact dynamics, J. Mech. Transm. Autom. Des. 109 (1987) 189–196.
- [17] *J. Bruyère, X. Gu, Ph. Vélez*, On the analytical definition of profile modifications minimising transmission error variations in narrow-faced spur helical gears, Mechanism and Machine Theory 92 (2015) 257-272
- [18] *T. Jabbour, G. Asmar*, Tooth stress calculation of metal spur and helical gears, Mechanism and Machine Theory 92 (2015), 375-390
- [19] *M. Barbieri, A. Zippo, F. Pellicano*, Adaptive grid-size finite element modeling of helical gear pairs, Mechanism and Machine Theory, 82(2014) 17-32